CHEMISTRY OF MATERIALS

Communication

pubs.acs.org/cm

Emission-Tunable Near-Infrared Ag_2S Quantum Dots

Peng Jiang,[†] Zhi-Quan Tian,[†] Chun-Nan Zhu, Zhi-Ling Zhang, and Dai-Wen Pang*

Key Laboratory of Analytical Chemistry for Biology and Medicine (Ministry of Education), College of Chemistry and Molecular Sciences, Research Center for Nanobiology and Nanomedicine (MOE 985 Innovative Platform), State Key Laboratory of Virology, and Wuhan Institute of Biotechnology, Wuhan University, Wuhan, 430072, P. R. China

Supporting Information

KEYWORDS: *luminescence, quantum dots, near-infrared, emission-tunable, silver sulfide*

Near-infrared (NIR) fluorescent quantum dots (QDs) are of great interest for the study of nanodiagnostics and imaging in vivo, because the fluorescence they emit could penetrate deeply into the body and is poorly absorbed by hemoglobin and water in the body.[1] Previous works on NIR fluorescent QDs were mainly focused on II–VI (CdTe),[2] IV–VI (PbS),[3] III–V (InAs),[4] and type-II heterostructured (CdTe/CdSe, CdSe/ZnTe, and CdSe/CdTe)[5] QDs with narrow band gaps. However, the intrinsic toxicity[6] of the above NIR quantum dots (QDs) from Cd(II), Pb(II), or As(III) restricts their further applications in biosystems. Thus, ternary I–III–VI NIR QDs (Cu–In–Se, $CuInS_2$, $AgInS_2$)[7] without intrinsic toxicity have recently been synthesized. However, it is tedious to tune their chemical composition, which is an important factor in controlling the optical properties of ternary I–III–VI QDs.

With a bulk band gap of 0.9–1.1 eV[8] and negligible toxicity,[8b,9] nanoscale α-Ag_2S is a potential candidate for NIR QDs, which is desirable for the use of imaging in vivo. Several reports on Ag_2S nanocrystals have been published,[8b,10] but only a few of them reported the NIR photoluminescent properties.[8b,10e] Moreover, to our knowledge, there is no report on tuning the fluorescence emissions of Ag_2S QDs in the NIR region, which are requisite for multicolor imaging in vivo. In this work, emission-tunable NIR Ag_2S QDs covering from 690 to 1227 nm were successfully synthesized, and the synthesized Ag_2S QDs could be transferred to water easily through ligand exchange.

A two-step procedure was applied to prepare different-sized Ag_2S QDs (Scheme 1). Small-sized Ag_2S QDs were synthesized

Scheme 1. Synthesis of Photoluminescence-Tunable NIR Ag_2S QDs

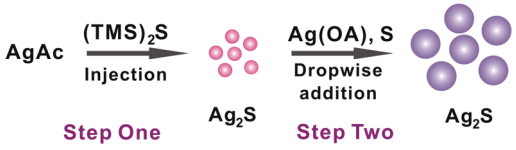

by injecting hexamethyldisilathiane ($(TMS)_2S$) into the mixture of silver acetate (AgAc), myristic acid (MA), 1-octylamine (OA), and 1-octadecene at a given temperature under argon flow. Large-sized Ag_2S QDs were prepared by seed-mediated growth, namely, by dropwise adding of Ag(OA) solution ($AgNO_3$ and OA dissolved in toluene) and sulfur solution (sulfur powder dissolved in toluene) into a toluene solution containing small-sized Ag_2S QDs.

TEM images (Figure 1A) of products synthesized in step one suggested that the products were spherical particles of 1.5 ± 0.4

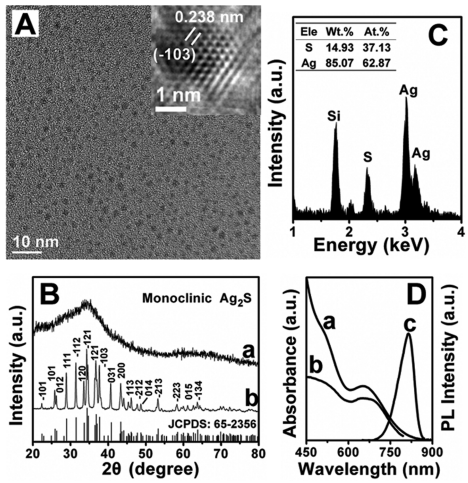

Figure 1. TEM image (A), IFFT-HRTEM image (A, inset) of Ag_2S nanocrystals synthesized in step one; XRD patterns of the 1.5 nm Ag_2S nanocrystals before (B, a) and after (B, b) thermal treatment at 180 °C under Ar flow for 1 h; EDX spectrum (C), absorption spectrum (D, a), excitation spectrum (D, b), and photoluminescence (PL) spectrum (D, c) of Ag_2S nanocrystals synthesized in step one.

nm in diameter and had a narrow size distribution (Supporting Information, Figure S1). The inverse fast Fourier transform (IFFT) HRTEM image (Figure 1A, inset) showed that the nanoparticles had clear crystal structures and obvious atomic planes. The atomic planes with *d*-spacing of 0.238 nm in the nanocrystals could be indexed as $(\bar{1}03)$ facet of monoclinic α-Ag_2S. The $(\bar{1}03)$ ring of monoclinic α-Ag_2S was also clearly observed in the selected area electron diffraction (SAED) results (Supporting Information, Figure S2), according with the

Received: August 26, 2011
Revised: November 28, 2011
Published: December 7, 2011

HRTEM results. Powder X-ray diffraction (XRD) results of the as-prepared Ag_2S nanocrystals synthesized in step one showed weak and undistinguishable diffraction peaks (Figure 1B(a)), which may be attributed to their small sizes and amorphous surface ligands. After a thermal treatment at 180 °C under Ar flow for 1 h, the XRD spectrum (Figure 1B(b)) was great improved[11] and matched well with monoclinic Ag_2S (JCPDS Card No. 65-2356). Energy-dispersive X-ray (EDX) data (Figure 1C) confirmed that the products consisted of elements Ag and S with the atomic ratio of Ag:S equaling to 1.7:1, which was close to the stoichiometry of bulk Ag_2S. The signal of element Si may be derived from the Si in the reaction precursor $(TMS)_2S$. FTIR spectrum confirmed that the nanocrystals were capped with OA and MA (Supporting Information, Figure S3). Thus, it could be concluded that the products synthesized in step one were indeed monoclinic α-Ag_2S nanocrystals.

UV−vis, photoluminescence (PL), and PL excitation (PLE) spectra of the synthesized Ag_2S nanocrystals were recorded (Figure 1D). As a consequence of quantum confinement, the first exciton peak appeared at 655 nm (1.9 eV) in the UV−vis spectrum, which was obviously blue-shifted compared with the band gap of bulk Ag_2S (0.9−1.1 eV). The PLE spectrum also displayed a well-defined exciton peak, which agreed well with the UV−vis spectrum. The room temperature PL emission peak of such 1.5 nm Ag_2S nanocrystals in *n*-hexane solution was located at 813 nm with a full width at half-maximum (fwhm) of 65 nm. The PL quantum yield was 0.18% (Supporting Information, Figure S4, using indocyanine green (ICG) as a reference standard, QY = 13% in DMSO). The fluorescence decay kinetics were found to be multiexponential with an average lifetime of 57 ns, which may be ascribed to the inhomogeneities of the nanocrystal surface (Supporting Information, Figure S5).[12]

It is known from previous reports[13] that the formation of monodisperse colloidal nanocrystals involves two steps called "nucleation" and "growth", and the balance between the nucleation and growth plays a key role in the synthesis of monodisperse nanocrystals.[13d,14] After the monomers are consumed rapidly to form nuclei in the initial nucleation process, the concentration of residual monomers in solution will affect the growth of the nanoparticles.[13b,15] Lower residual monomer concentration in solution after nucleation would slow down the growth rate. Injection and growth temperatures, which were crucial factors to tune the balance between the nucleation and growth,[16] were varied to modulate the formation process of the Ag_2S nanocrystals. With injection temperature higher than 90 °C, the initial nucleation rate was so fast that the absorption peak and PL emission peak appeared nearly immediately after the injection of $(TMS)_2S$ and did not shift obviously with the increased growth time (Supporting Information, Figure S6). This phenomenon could be attributed to the complete depletion of highly reactive $(TMS)_2S$ following nucleation and their lack at the further growth stage, just as previously reported strategies for synthesizing InP and Cd_3As_2 nanocrystals using $(TMS)_3P$ and $(TMS)_3As$ as phosphorus precursor and arsenic precursor.[17] Figure 2 showed temporal evolution of the absorption spectra of Ag_2S nanocrystals synthesized at different injection/growth temperatures. With the injection/growth temperature set at 50 °C/50 °C, the absorption spectrum varied from shouldering at 520 nm to peaking at 590 nm by increasing the growth time from 5 s to 30 min (Figure 2A), because a smaller amount of precursors reacted to produce nuclei in the initial stage at lower

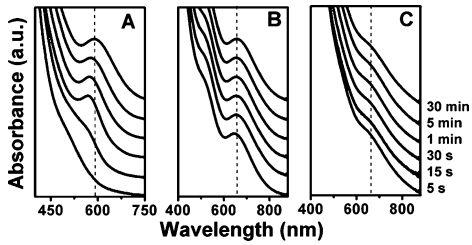

Figure 2. Temporal evolution of absorption spectra of Ag_2S nanocrystals (dispersed in hexane) synthesized at different injection/growth temperatures, (A) 50 °C/50 °C, (B) 90 °C/70 °C, and (C) 120 °C/90 °C.

temperature and the excess monomers reacted at the further growth stage. In comparison, no obvious absorption peak shift was observed when the injection/growth temperature was set at 90 °C/70 °C or 120 °C/90 °C (Figure 2B,C), as mentioned above in the text. By modulating the injection temperature and the growth time, the PL emission peak of the nanocrystals could be tuned from 690 to 820 nm (Figure 3).

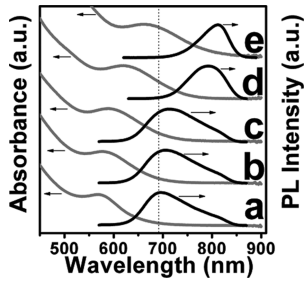

Figure 3. PL spectra and corresponding absorption spectra of Ag_2S nanocrystals (in hexane) synthesized under different conditions. Injection temperature: 50 °C, growth time: 30 s (a), 5 min (b) and 30 min (c); Injection temperature: 80 °C, growth time: 5 s (d); Injection temperature: 110 °C, growth time: 5 s (e). (The tails of spectra d and e may be influenced by the spectral range (290−850 nm) of the PMT detector).

Besides modulating the temperature and growth time, ligand concentration is another important factor to tune the size and PL of synthesized nanoparticles.[6b,18] However, Ag_2S nanocrystals with emission above 820 nm were also not obtained by varying ligand concentration in step one. Therefore, a seed-mediated growth method (step two), which had been proven to be an available strategy to synthesize larger sized monodisperse nanoparticles,[19] was employed. Ag_2S nanocrystals with emission above 820 nm were successfully obtained. After the seed-mediated growth for 18 h, the size of the Ag_2S nanocrystals increased from 1.5 to 4.6 nm (Figure 4A and

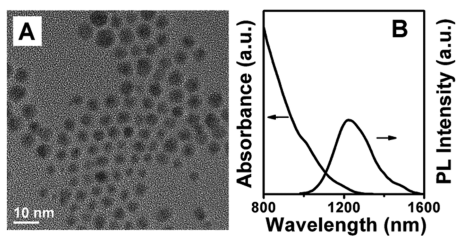

Figure 4. (A) TEM image and (B) absorption and PL spectra of Ag_2S nanocrystals (in tetrachloroethylene) synthesized in step two.

Supporting Information, Figure S7), and the PL emission peak red-shifted from 813 nm to 1227 nm (Figure 4B). Instead of a distinguishable absorption peak, an absorption shoulder at 1010 nm was shown in the NIR absorption spectrum (Figure 4B). XRD (Supporting Information, Figure S8) and EDX (Supporting Information, Figure S9) results confirmed that the products synthesized in step two were also monoclinic α-Ag_2S nanocrystals. It should be pointed out that step two must be performed at room temperature by using lowly reactive sulfur powder as sulfur precursors and using a dropwise addition manner to suppress the continuous nucleation.

For use in biology, nanoparticles synthesized in organic solvent must be transferred to water phase. Surface ligand exchange is a convenient method to realize the transfer.[20] Alkanethiolates with carboxylic acid (COOH) terminal groups were used to replace the surface ligand of the as-prepared Ag_2S nanocrystals, and the Ag_2S nanocrystals were well dispersed in water (Supporting Information, Figure S10). Evidently, the PL properties of the Ag_2S nanocrystals were well retained (QY = 0.15%) and were photostable after the transfer (Supporting Information, Figure S10).

In summary, emission-tunable NIR Ag_2S nanocrystals with sizes ranging from below 1.5 to 4.6 nm have been successfully synthesized. The photoluminescence covers a range from 690 to 1227 nm. The initial injection temperature and growth time play key roles in tuning the PL emissions of Ag_2S nanocrystals. With lower initial injection temperature, fewer monomers are consumed to form initial nuclei and more monomers remain for the growth process. Thus, the PL emissions shift obviously to red by increasing the growth time. The emission-tunable NIR Ag_2S nanocrystals have great potential for the study of multiple nanodiagnostics and multicolor imaging in vivo.

■ ASSOCIATED CONTENT

Ⓢ Supporting Information

Experimental details, size distribution histograms, SAED, FTIR spectrum, PL decay data UV−vis absorption, PL spectra, XRD, and EDX of Ag_2S QDs (PDF). This material is available free of charge via the Internet at http://pubs.acs.org.

■ AUTHOR INFORMATION

Corresponding Author

*E-mail: dwpang@whu.edu.cn.

Author Contributions

†These authors contributed equally.

■ ACKNOWLEDGMENTS

This work was supported by the National Basic Research Program of China (973 Program, Nos. 2011CB933600 and 2006CB933100), the Science Fund for Creative Research Groups of NSFC (Nos. 20921062 and 20621502), the National Natural Science Foundation of China (20833006; 21005056), and the "3551 Talent Program" of the Administrative Committee of East Lake Hi-Tech Development Zone ([2011]137).

■ REFERENCES

(1) Weissleder, R. *Nat. Biotechnol.* **2001**, *19*, 316−317.

(2) Yu, W. W.; Wang, Y. A.; Peng, X. G. *Chem. Mater.* **2003**, *15*, 4300−4308.

(3) Hines, M. A.; Scholes, G. D. *Adv. Mater.* **2003**, *15*, 1844−1849.

(4) Cao, Y. W.; Banin, U. *J. Am. Chem. Soc.* **2000**, *122*, 9692−9702.

(5) (a) Kim, S.; Fisher, B.; Eisler, H. J.; Bawendi, M. *J. Am. Chem. Soc.* **2003**, *125*, 11466−11467. (b) Blackman, B.; Battaglia, D. M.; Mishima, T. D.; Johnson, M. B.; Peng, X. *Chem. Mater.* **2007**, *19*, 3815−3821.

(6) (a) Gao, J.; Chen, K.; Xie, R.; Xie, J.; Yan, Y.; Cheng, Z.; Peng, X.; Chen, X. *Bioconjugate Chem.* **2010**, *21*, 604−609. (b) Xie, R.; Battaglia, D.; Peng, X. *J. Am. Chem. Soc.* **2007**, *129*, 15432−15433.

(7) (a) Allen, P. M.; Bawendi, M. G. *J. Am. Chem. Soc.* **2008**, *130*, 9240−9241. (b) Xie, R. G.; Rutherford, M.; Peng, X. G. *J. Am. Chem. Soc.* **2009**, *131*, 5691−5697.

(8) (a) Meherzi-Maghraoui, H.; Dachraoui, M.; Belgacem, S.; Buhre, K. D.; Kunst, R.; Cowache, P.; Lincot, D. *Thin Solid Films* **1996**, *288*, 217−223. (b) Du, Y. P.; Xu, B.; Fu, T.; Cai, M.; Li, F.; Zhang, Y.; Wang, Q. B. *J. Am. Chem. Soc.* **2010**, *132*, 1470−1471.

(9) Nowack, B. *Science* **2010**, *330*, 1054−1055.

(10) (a) Gao, F.; Lu, Q. Y.; Zhao, D. Y. *Nano Lett.* **2003**, *3*, 85−88. (b) Wang, D. S.; Xie, T.; Peng, Q.; Li, Y. D. *J. Am. Chem. Soc.* **2008**, *130*, 4016−4022. (c) Yang, J.; Ying, J. Y. *Chem. Commun.* **2009**, 3187−3189. (d) Sahu, A.; Qi, L. J.; Kang, M. S.; Deng, D. N.; Norris, D. J. *J. Am. Chem. Soc.* **2011**, *133*, 6509−6512. (e) Yarema, M.; Pichler, S.; Sytnyk, M.; Seyrkammer, R.; Lechner, R. T.; Fritz-Popovski, G.; Jarzab, D.; Szendrei, K.; Resel, R.; Korovyanko, O.; Loi, M. A.; Paris, O.; Hesser, G.; Heiss, W. *ACS Nano* **2011**, *5*, 3758−3765.

(11) Carenco, S.; Resa, I.; Le Goff, X.; Le Floch, P.; Mézailles, N. *Chem. Commun.* **2008**, 2568.

(12) Wang, H.; de Mello Donegá, C.; Meijerink, A.; Glasbeek, M. *J. Phys. Chem. B* **2005**, *110*, 733−737.

(13) (a) Murray, C. B.; Norris, D. J.; Bawendi, M. G. *J. Am. Chem. Soc.* **1993**, *115*, 8706−8715. (b) Peng, X.; Wickham, J.; Alivisatos, A. P. *J. Am. Chem. Soc.* **1998**, *120*, 5343−5344. (c) Qu, L.; Yu, W. W.; Peng, X. *Nano Lett.* **2004**, *4*, 465−469. (d) Ji, X.; Song, X.; Li, J.; Bai, Y.; Yang, W.; Peng, X. *J. Am. Chem. Soc.* **2007**, *129*, 13939−13948.

(14) Yu, W. W.; Peng, X. *Angew. Chem., Int. Ed.* **2002**, *41*, 2368−2371.

(15) Yin, Y.; Alivisatos, A. P. *Nature* **2005**, *437*, 664−670.

(16) Shevchenko, E. V.; Talapin, D. V.; Schnablegger, H.; Kornowski, A.; Festin, Ö.; Svedlindh, P.; Haase, M.; Weller, H. *J. Am. Chem. Soc.* **2003**, *125*, 9090−9101.

(17) (a) Allen, P. M.; Walker, B. J.; Bawendi, M. G. *Angew. Chem., Int. Ed.* **2010**, *49*, 760−762. (b) Harris, D. K.; Allen, P. M.; Han, H.-S.; Walker, B. J.; Lee, J.; Bawendi, M. G. *J. Am. Chem. Soc.* **2011**, *133*, 4676−4679.

(18) Xie, R. G.; Zhang, J. X.; Zhao, F.; Yang, W. S.; Peng, X. G. *Chem. Mater.* **2010**, *22*, 3820−3822.

(19) (a) Sun, S. H.; Zeng, H.; Robinson, D. B.; Raoux, S.; Rice, P. M.; Wang, S. X.; Li, G. X. *J. Am. Chem. Soc.* **2004**, *126*, 273−279. (b) Brown, K. R.; Walter, D. G.; Natan, M. J. *Chem. Mater.* **2000**, *12*, 306−313.

(20) Zhao, X.; Cai, Y.; Wang, T.; Shi, Y.; Jiang, G. *Anal. Chem.* **2008**, *80*, 9091−9096.